J Mater Sci (2010) 45:112–117
DOI 10.1007/s10853-009-3899-4

CdS_xSe_{1-x} quantum dots studied through optical absorption, steady-state photoluminescence, and resonant Raman spectroscopies

B. Can Ömür · A. Aşıkoğlu · Ç. Allahverdi · M. H. Yükselici

Received: 19 June 2009 / Accepted: 15 September 2009 / Published online: 26 September 2009

Abstract CdS_xSe_{1-x} nanoparticles or quantum dots (QDs) were grown in borosilicate glass by a two-step heat-treatment process from a melt-quenched color filter glass. We incorporate the results of optical absorption, steady-state photoluminescence (PL), and resonant Raman spectroscopies in the study of growth kinetics of CdS_xSe_{1-x} QDs. A modeling of PL spectra employing two Gaussian emission bands and a quantized-state effective mass model in the strong confinement regime reveals that (i) the average particle size ranges from 1.7 to 8.5 nm, (ii) the size dispersion narrows down to 0.22 nm for a single sample, and (iii) QDs form by diffusion-limited growth. We presume that size-dependent higher energy PL band close to the asymptotic absorption edge is due to surface-assisted electron-hole recombination since the difference between optical absorption and PL bands decreases from 239 to 122 meV with increasing average radius.

Introduction

II–VI semiconductor nanocrystals, often called quantum dots (QDs) have been scrutinized for a quarter century due to their potential applications as nonlinear optical devices in optoelectronics, fluorescent labels in bioengineering, and window materials in solar cells [1–5]. Nanometer-sized crystals have distinctive optical properties due to the confinement of charged particles in all three space dimensions. The band gap can be modified to optimize the optical properties of the nanostructure by controlling the size. Solid phase precipitation of CdS_xSe_{1-x} QDs in glass has been a well-established technique to produce stable nanocrystals at temperatures below 250 °C [6]. Confinement of charged particles has been studied through linear/nonlinear optical methods and structural characterizations such as TEM and SAXS [2, 3, 6–8]. Previous optical studies on CdS_xSe_{1-x} QDs mostly model the first exciton peak in optical absorption spectra to estimate size and size dispersion of nanocrystals [9–11] while steady-state photoluminescence spectroscopy has been reserved for investigating trap states [12–15].

In this work we grow different size CdS_xSe_{1-x} QDs in glass by solid-phase precipitation. Present work differs from previous studies in that we incorporate the results of optical absorption (ABS), steady-state photoluminescence (PL), and resonant Raman spectroscopies in the study of growth kinetics of CdS_xSe_{1-x} QDs. We simulate PL spectra to predict the average size of nanocrystals and size dispersion, and to understand the evolution of trap states with the help of ABS spectroscopy. We present both progression of coloring of the samples and blue-shift of the lowest transition energy in ABS spectrum with heat-treatment time and temperature. We monitor the composition of QDs during growth through resonant Raman spectroscopy.

Sample preparation and experimental results

Our starting material to grow CdS_xSe_{1-x} QDs is commercially available color filter RG695 Schott borosilicate glass doped with $CdS_{.08}Se_{.92}$ as reported in Ref. [7]. We first melt as-received glass at about 1000 °C for 15 min to dissolve the particles and quench the melt rapidly to room

B. Can Ömür · A. Aşıkoğlu · Ç. Allahverdi · M. H. Yükselici (✉)
Department of Physics, Faculty of Arts and Sciences, Yıldız Technical University, Davutpaşa-Topkapı, 34010 Istanbul, Turkey
e-mail: yukseli@yildiz.edu.tr

temperature and then anneal the glass at 450 °C for 5 h (primary heat treatment) to relieve stress in glass and to initiate nucleation and finally anneal the glass at different temperatures around glass transition temperature for different periods of times (secondary heat treatment) to grow nanoparticles. Samples are numbered according to secondary heat-treatment temperature and time as shown in the first three columns of Table 1. The fourth and last columns show average nanocrystal radius and size dispersion, respectively, calculated by simulating the PL spectra presented in the next section. The fifth column includes nanocrystal radius calculated from the energetic position of the first exciton peak in Fig. 1 according to Eq. 2 given in the next section.

We present optical absorption spectra and the progression of coloring of the samples in Fig. 1. As the color progresses or as QDs grow, an absorption peak (or first exciton peak due to transition from a hole state to an electron state) appears. This peak is due to the absorption of light by QDs. Its height is proportional to the volume fraction of nanocrystals, its shift in wavelength to the square of average nanocrystal radius and its full width at half maximum to the size dispersion. The lowest transition energy for the bulk crystal is blue shifted when the size is reduced which is due to quantum confinement effect. As seen in Fig. 1, a shift of ~200 nm in the first exciton peak position was observed with heat-treatment temperature and time. In general we may say that the longer the heat-treatment time or the higher the temperature the larger the nanocrystals are grown. After long time thermal treatment at a given temperature, the optical absorption band edge approaches to that of bulk crystal of the same composition as shown in Fig. 1.

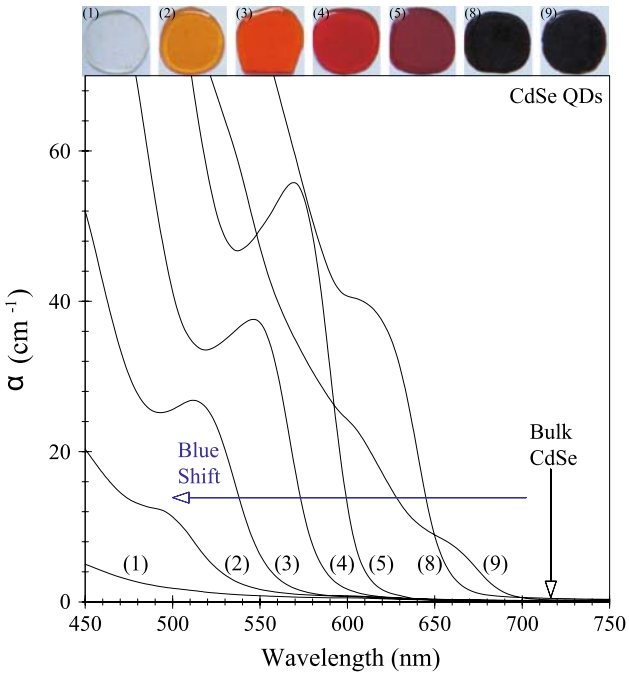

Fig. 1 Optical absorption spectra for as-received color filter glass doped with $CdS_{.08}Se_{.92}$ melted at ~1000 °C for 15 min, heat treated at 450 °C for 5 h (primary heat treatment) and finally heat treated at different temperatures for different periods of times (secondary heat treatment). The colors of samples are presented at *top* of the figure. See Table 1 for the details. Secondary heat-treatment temperatures and times are numbered as follows, in °C and in h, respectively: (*1*) 600, ½; (*2*) 625, 1; (*3*) 625, 2; (*4*) 625, 4; (*5*) 625, 8; (*6*) 650, 2; (*7*) 650, 4; (*8*) 650, 8, (*9*) 675, 2; (*10*) 675, 4

Table 1 Samples numbered according to the secondary heat-treatment temperature and time

Sample number	Secondary annealing temperature (°C)	Time (h)	R_0* (nm)	R_0** (nm)	σ_R* (nm)
1	600	½	–	–	–
2	625	1	1.7 ± 0.38	2.1	1.2 ± 0.3
3	625	2	1.8 ± 0.36	2.2	1.3 ± 0.3
4	625	4	2.9 ± 0.10	2.5	0.32 ± 0.01
5	625	8	3.3 ± 0.73	2.7	0.22 ± 0.05
6	650	2	3.4 ± 0.17	3.1	0.55 ± 0.03
7	650	4	4.3 ± 0.87	3.4	0.70 ± 0.14
8	650	8	4.8 ± 0.17	3.5	0.70 ± 0.03
9	675	2	7.2 ± 0.57	4.5	1.3 ± 0.1
10	675	4	8.5 ± 1.3	4.7	1.3 ± 0.2

Average radius (R_0*) and size dispersion (σ_R*) extracted by simulating the PL spectra presented in Fig. 3a. Average radius (R_0**) calculated from the energetic position of first exciton peak is presented for comparison

Resonant Raman scattering measurements were carried out at room temperature on Renishaw 250 mm focal length in Via Reflex Spectrometer System using Rayleigh line rejection filter allowing Raman spectrum to 100 cm^{-1} from the laser line. The resonant Raman spectra excited by Ar^+ laser at 514.5 nm is shown in Fig. 2. Heat-treatment time and/or temperature increase from top to bottom. The peak at 206 cm^{-1} is due to zone-center LO phonon of CdS_xSe_{1-x} mode and peak position does not shift with time or/and temperature. We present normalized steady-state PL spectra excited by cw Ar^+ laser of the intensity of ~70 mW/mm^2 at 488 nm in Fig. 3a and the modeling of PL spectra in Fig. 3b. Details of PL and optical transmission measurements have been reported in a previously published paper of ours [16].

Modeling of photoluminescence spectra

Previous studies on CdS_xSe_{1-x} nanocrystals show that the PL spectra generally display a two peak structure [17, 18].

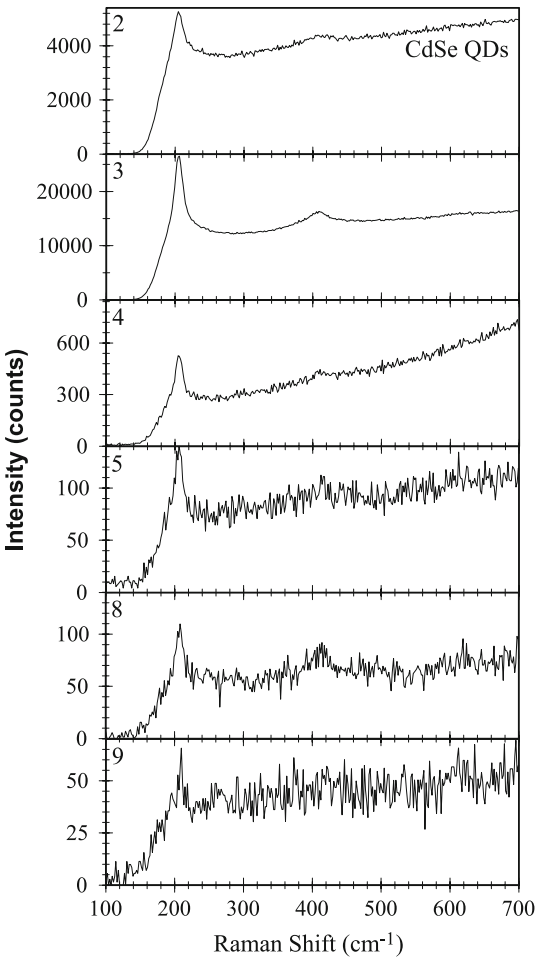

Fig. 2 Resonant Raman spectra excited at 514.5 nm for $CdS_{.08}Se_{.92}$ QDs in glass. Secondary heat-treatment temperatures and times are numbered as follows, in °C and in h, respectively: (*2*) 625, 1; (*3*) 625, 2; (*4*) 625, 4; (*5*) 625, 8; (*8*) 650, 8, (*9*) 675, 2

The higher energy peak close to the asymptotic absorption edge is assumed to be due to electron-hole recombination and the other low energy peak due to deep trap levels. We therefore employ a two term function to model the PL spectra, which was described in Ref. [19]. The calculated PL intensity is of the form,

$$I_{\mathrm{PL}}(h\nu) = \frac{A}{\sqrt{2\pi}\Gamma_{\mathrm{trap}}} \exp\left[-\frac{(h\nu - E_{\mathrm{trap}})^2}{2\Gamma_{\mathrm{trap}}^2}\right] + \sum_R \left\{ \frac{1}{\sqrt{2\pi}\sigma_{\mathrm{R}}} \exp\left[-\frac{(R-R_0)^2}{2\sigma_{\mathrm{R}}^2}\right] \frac{B}{\sqrt{2\pi}\Gamma} \exp\left[-\frac{(h\nu - E_{\mathrm{R}})^2}{2\Gamma^2}\right] \right\} \quad (1)$$

where A and B are constants, R_0 the average radius of the ensemble of nanocrystals, σ_{R} the standard deviation of the radius, $\Gamma = 2\%$ the width in percent of homogeneous broadening, and $\Gamma_{\mathrm{trap}} = 10$–$20\%$ the width in percent of trap band broadening. We note that $\Gamma = (\Delta E/E) \times 100$, where ΔE is the standard deviation of homogeneous (or trap band broadening) at an energy of E. E_{R} is the size-dependent first exciton transition energy given by [20],

$$E_{\mathrm{R}}(\mathrm{eV}) = E_{\mathrm{g}}(\mathrm{eV}) - \frac{0.14}{R(\mathrm{nm})} + \frac{0.356}{\mu[R(\mathrm{nm})]^2} \quad (2)$$

where the first term is the bulk band gap of $CdS_{.08}Se_{.92}$ crystal of $E_{\mathrm{g}} = 1.727$ eV, the second term Coulomb potential energy between an electron and a hole, and the third term confinement energy for an electron and a hole. $\mu = 0.106$ is the reduced mass of an electron-hole pair in units of electron rest mass m_0. It should be noticed that $CdS_{.08}Se_{.92}$ QDs grown in a glass matrix by solid phase precipitation undergo a compressive strain due to the thermal mismatch between the nanocrystal and the matrix. However, previous studies on similar systems show that the pressure-induced gap increment $\Delta E_{\mathrm{g}}^{\mathrm{p}}$ is in the order of meV and can therefore be negligible [21].

Each PL spectrum in Fig. 3a was taken separately and modeled according to Eq. 1, and the best-fit parameters for R_0, σ_{R}, and E_{trap} were determined. In Fig. 4 average nanocrystal radius is plotted against the square root of heat-treatment time. The straight lines are the linear fits at each heat-treatment temperature. This is consistent with the diffusion-limited growth which predicts a linear relation between the average radius and the square root of heat-treatment time. Size dispersion (σ_{R}) is plotted against the square root of heat-treatment time in Fig. 5. Size dispersion gets its lowest value of 0.22 nm at the end of heat-treatment time of 8 h at 625 °C. The trap band energy is plotted as function of heat-treatment time for each temperature in Fig. 6. The trap band energy remains constant at around 1.8 eV independent of both heat-treatment time and temperature. In Fig. 7 we plot the difference between the energetic positions of ABS and higher energy PL bands against the average radius. The details for the samples are given in Table 1.

Discussion

We discuss the resonant Raman spectra in Fig. 2 with the help of optical absorption spectra in Fig. 1. The strong asymmetry of the background intensity toward higher wavelengths in the Raman spectra is presumed to be due to the PL from the sample. Raman scattering can be used as a compositional probe of II–VI ternary semiconductor nanocrystals [22]. The peak near 200 cm^{-1} is due to zone-center LO phonons of CdSe-like modes in nanocrystals. The frequency of phonon vibration depends on the stoichiometry of the compound. We hence conclude that the composition does not change with the growth of QDs since the LO peak does not shift in wave-number.

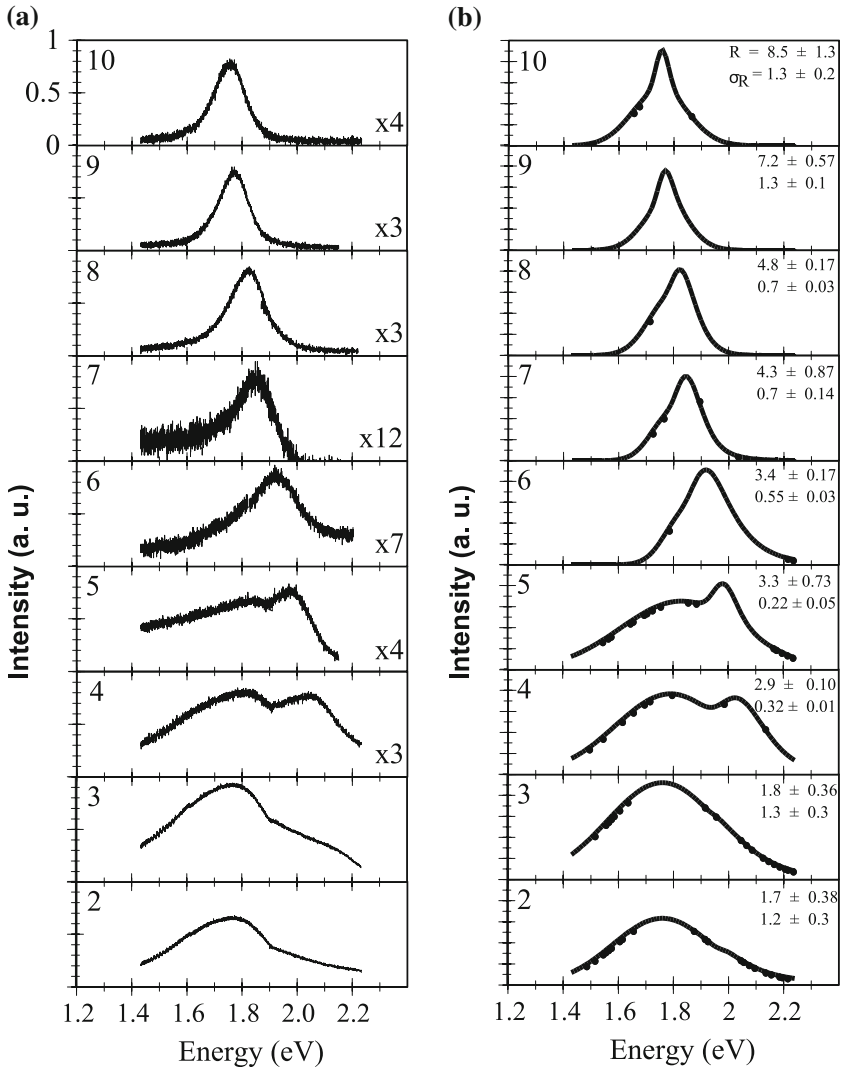

Fig. 3 **a** Steady-state photoluminescence (PL) spectra for $CdS_{.08}Se_{.92}$ QDs in glass excited by cw Ar^+ laser of the intensity of ~70 mW/mm^2 at 488 nm. **b** Simulated PL spectra. Best-fit parameters for average nanocrystal radius (R_0) and size dispersion (σ_R) presented at the upper right corner of each spectrum. Secondary heat-treatment temperatures and times are numbered as follows, in °C and in h, respectively: (*2*) 625, 1; (*3*) 625, 2; (*4*) 625, 4; (*5*) 625, 8; (*6*) 650, 2; (*7*) 650, 4; (*8*) 650, 8, (*9*) 675, 2; (*10*) 675, 4

The sample 3 has the highest intensity zone-center LO Raman peak (see Fig. 2 for sample 3) since Raman spectra are excited with a laser line of 514.5 nm which is resonant with the wavelength's position of first exciton band for this sample (see Fig. 1 for sample 3). As the nanocrystals grow the laser line stays away from the first exciton peak position and, as a result, Raman peak intensity diminishes and finally disappears with increasing time and/or temperature. We note that the intensity of zone-center LO phonon mode strongly depends on the resonance of excitation laser line with the energetic position of first exciton band in ABS spectra.

We discuss the PL spectra (see Fig. 3a) with the help of the modeling presented in the previous section (see Fig. 3b). At the early stages of growth, that is, for samples 2 and 3, a single peak at around 1.8 eV appears. We presume that this peak is due to volume traps and the modeling predicts that it is almost stationary. During the growth of QDs, a higher energy peak appears at around 2.1 eV for sample 4, grows and gradually shifts to lower energies for sample 5. As the heat treatment continues at higher temperatures for samples from 5 to 10 this higher energy peak overlaps with stationary trap band. The modeling suggests that this is a size-dependent band. We identify this higher energy peak as a surface-assisted electron-hole recombination band because (i) it is red shifted from the first exciton band by greater than 120 meV and (ii) the amount of red shift decreases with size as seen in Fig. 7, which is expected since surface to volume ratio of a nanocrystal decreases as $1/R$ with size. In a previous study [23] on $CdS_{.08}Se_{.92}$ QDs precipitated in RG695 Schott glass, steady-state PL spectra excited at 337 nm displays a one-peak structure at ~1.8 eV where the higher energy PL peak could not be resolved. The number of peaks resolved in PL spectra depends on the excitation energy [24]. QDs whose size-dependent band gap energy is above the excitation energy will not contribute to the PL intensity.

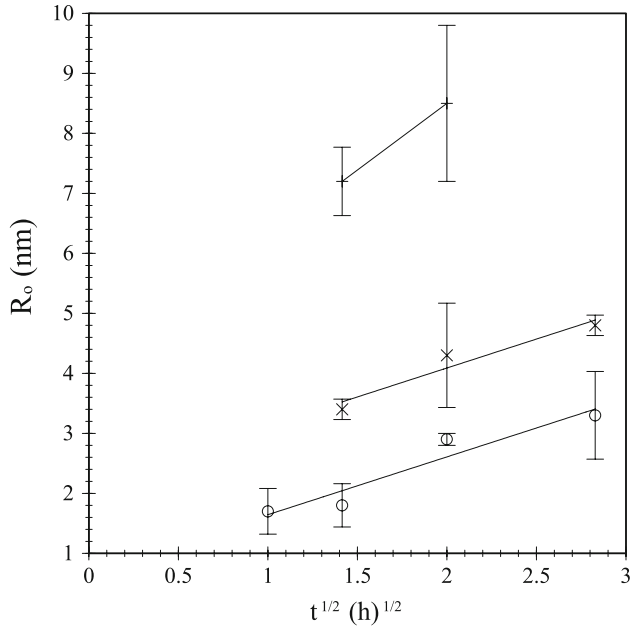

Fig. 4 Average nanocrystal radius plotted against the square root of heat-treatment time for samples heat treated secondarily at 625 °C (*open circle*), 650 °C (*times*), and 675 °C (*plus*). The *straight lines* are the linear fits

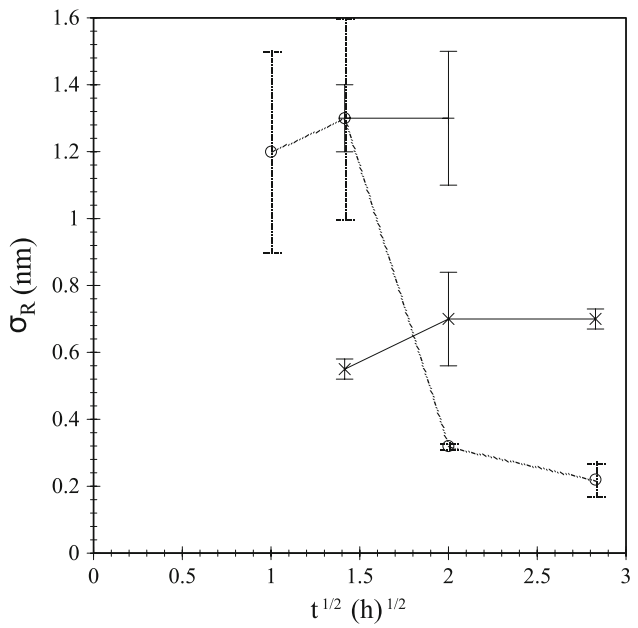

Fig. 5 Size dispersion (σ_R) plotted against the square root of heat-treatment time for samples heat treated secondarily a 625 °C (*open circles*), 650 °C (*times*), and 675 °C (*plus*). The *lines* between data points are for the eye to follow

We also note that the energetic position of the first exciton peak in the optical absorption spectrum underestimates the average radius of the particles compared to the average particle's radius calculated by simulating the PL spectrum as seen in Table 1. This is quite normal since the

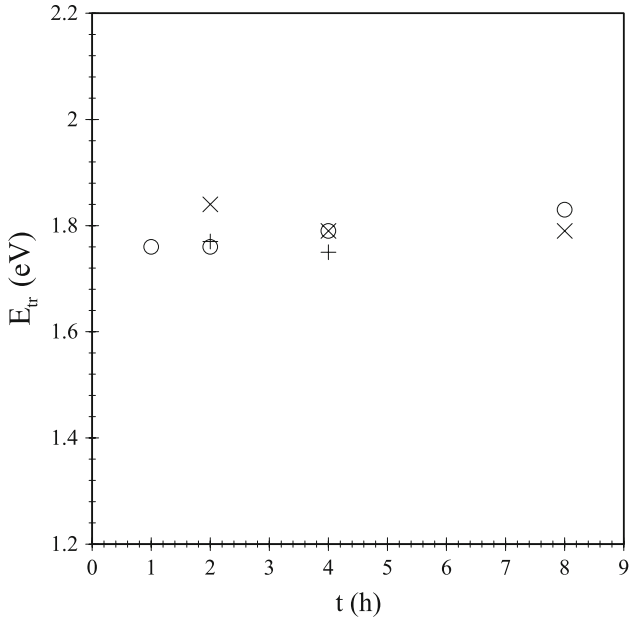

Fig. 6 Trap state energy determined through modeling of PL spectra plotted as a function of heat-treatment time for samples heat treated secondarily at 625 °C (*open circle*), 650 °C (*times*), and 675 °C (*plus*)

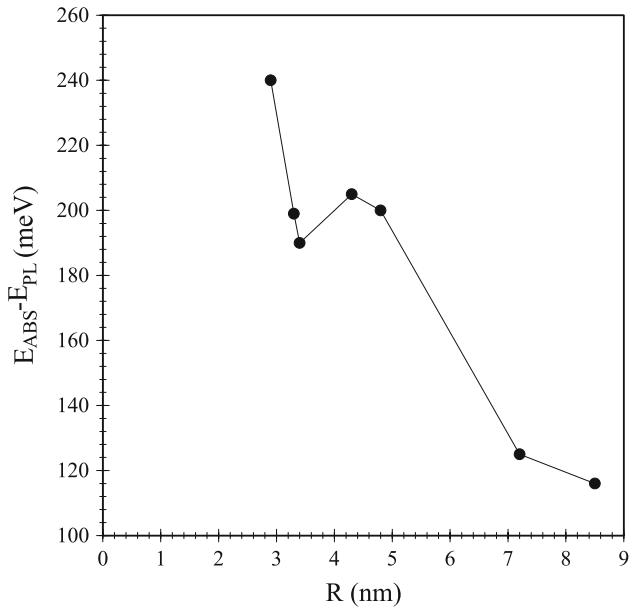

Fig. 7 Difference between the energetic positions of absorption and photoluminescence bands against the average nanocrystal radius. The *lines* between data points are for the eye to follow

PL peak is red shifted with respect to the first exciton peak and the amount of shift decreases with increasing radius as seen in Fig. 7. However, for technological applications, it is important to know how the PL energy depends on size and size distribution of QDs since CdS_xSe_{1-x} QDs can be used as luminescent labels in bioengineering.

Summary

Different size $CdS_{.08}Se_{.92}$ nanocrystals were grown in glass through a two-step heat-treatment process. Size-induced shift of $\sim$200 nm in the first exciton peak position in optical absorption spectrum (ABS) was observed. A modeling of steady-state PL spectra with a combination of a Gaussian trap state emission band and a size-dependent Gaussian like recombination band with the help of a quantized-state effective mass model in the strong confinement limit leads to the following predictions: (i) the average nanocrystal radius ranges from 1.7 to 8.5 nm, (ii) the size dispersion narrows down to 0.22 nm for a single sample, and (iii) nanocrystals form by diffusion-limited growth. The evolution of Raman spectra with heat-treatment time and temperature shows that the intensity of zone-center LO phonon mode strongly depends on the resonance of excitation laser line energy with the energetic position of first exciton band in ABS spectra. We presume that size-dependent higher energy PL band close to the asymptotic absorption edge is due to surface-assisted electron-hole recombination since the difference between ABS and PL bands decreases from 239 to 122 meV with increasing size.

Acknowledgements This work is supported by Yıldız Technical University Research Project Coordination under project nos. 23-01-01-01 and 24-01-01-03 and partly by TUBITAK under the project no. TBAG-AY/378 (104T119). We thank M. Çulha for taking Raman spectra.

References

1. Ekimov AI, Onushchenko AA (1981) JETP Lett 34:345
2. Flytzanis C, Harbe F, Klein MC, Ricard D (1990) Optics in complex systems. SPIE, Bellingham, WA
3. Jain R, Lin RC (1983) J Opt Soc Am 73:647
4. Nozik AJ (2002) Physica E 14:115
5. Chan WCW, Maxwell DJ, Gao X, Bailey RE, Han M, Nie S (2002) Curr Opin Microbiol 13:40
6. Borelli NF, Hall DW, Holland HJ, Smith DW (1987) J Appl Phys 61:5399
7. Banfi G, Degiorgio V, Ricard D (1998) Adv Phys 47:447
8. Hayes TM, Lurio LB, Persans PD (2001) J Phys Condens Matter 13:425
9. Ekimov AI, Onushchenko AA (1982) Sov Phys Semicond 16:775
10. Fuyu Y, Parker JM (1988) Mater Lett 6:233
11. Yukselici MH (2002) J Phys Condens Matter 14:1153
12. Mei G, Carpenter S, Persans PD (1991) Solid State Commun 80:557
13. Stokes KL, Persans PD (1995) Mater Res Soc Symp Proc 358:241
14. Mei G (1992) J Phys Condens Matter 4:7521
15. Junior DRM, Qu F, Alcalde AM, Dantas NO (2003) Microelectron J 34:643
16. Yükselici MH, Allahverdi Ç (2008) J Lumin 128:537
17. Bawendi MG, Carroll PJ, Wilson WL, Brus LE (1992) J Chem Phys 96:946
18. Hache F, Klein MC, Ricard D, Flytzanis C (1991) J Opt Soc Am B 8:1802
19. Ravindran TR, Arora AK, Balamurugan B, Mehta BR (1999) Nanostruct Mater 11:603
20. Henneberger F, Puls J, Spiegelberg Ch, Schülzgen A, Rossman H, Jungnickel V, Ekimov AI (1991) Semicond Sci Technol 16:A41
21. Azhniuk Yu M, Lopushansky VV, Gomonnai VV, Yukhymchuk VO, Turok II, Studenyak Ya I (2008) J Phys Chem Sol 69:139
22. Tu A, Persans PD (1991) Appl Phys Lett 58:1506
23. Allahverdi Ç, Yükselici MH, Turan R, Seyhan A (2004) Semicond Sci Technol 19:1005
24. Rodrigues PAM, Tamulaitis G, Yu PY, Risbud SH (1995) Solid State Commun 94:583